© 2004 VSB-TUO, Ostrava, ISSN 1562-3580

Teaching and Design on Smart MEMS Pressure Sensor Module

Jium-Ming LIN
707 Sec. 2, Wu-Fu Rd., Department of Mechanical Engineering, Chung-Hua University, Hsin-Chu Taiwan, R. O. C. 30012, E-mail: jmlin@chu.edu.tw

KEYWORDS: *smart pressure sensor, MEMS, Wheatstone bridge*

ABSTRACT: *The purpose of this paper is to teach the senior students how to integrate the knowledge learning from the courses such as: electric circuits, electronics, microprocessor, semiconductor as well as MEMS fabrication process and package. The special topic of the experiment is to design a smart pressure sensor. Firstly, the smart sensor module architecture defined by IEEE 1451 Standard is introduced, which is obtained by using a single-chip 8051 microprocessor to calibrate the pressure sensor temperature biases and drift coefficients, and then store them to the on-chip memory for compensation. Thus the user can make the calibration and compensation through the command bus, which will make the sensor development much more easier, reliable and accurate.*

The second part is to fabricate the MEMS pressure sensor by the E-gun evaporator to deposit pressure-resistive film on a deformable membrane, and then using the photolithography processes to pattern it into a form of Wheatstone bridge. Thirdly, a pulsed-current source is introduced for the students to drive the bridge circuit, such that the temperature effects due to the power supply and the sensor can be reduced and compensated. Finally are the sensor module circuit design, layout and experiment. The output voltage of the pressure sensor is filtered first and then amplified by an instrumentation amplifier, an A/D converter is applied to convert the conditioned signal to a digital one, such that both the temperature bias and drift can be easily corrected by the microprocessor. The experiment results showed that the aforementioned designing and circuit processing are available and affordable.

1 INTRODUCTION

There are several methods for making the pressure sensor by using the effects such as piezo-resistive, magneto-resistive, pressure-capacitive, and pressure-resistive. Among these methods silicon is the most commonly used substrate material, and the MEMS technology is applied to make the diaphragm or membrane. The purpose of this teaching and research is to design a smart MEMS pressure sensor module. The pressure-resistive material of poly-Si is applied, and the resistors are arranged in a form of Wheatstone bridge on a deformable membrane. It is shown that the current source is better than voltage one to drive the bridged circuit for temperature and bias compensation. The differential output voltage is amplified first by an instrumentation amplifier and then convert it to a digital signal by a A/D converter, such that both the temperature effect and the bias can be compensated digitally by a 8051 microcomputer according to the IEEE 1451 standard.

2 PRINCIPLE OF WHEATSTONE BRIDGE PRESSURE SENSOR

The pressure-resistive bridged-type pressure sensor is shown in Fig.1, in which there are two p-type resistors *R1* and *R3* arranged in parallel to the two opposite-sides of the membrane as shown in Fig. 2, and the other two resistors *R2* and *R4* are arranged in perpendicular to the other sides of the membrane.

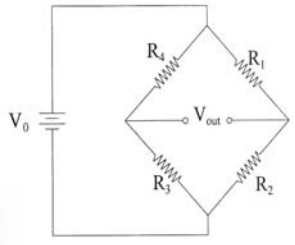

Figure 1 – Pressure-resistive bridged-type pressure sensor.

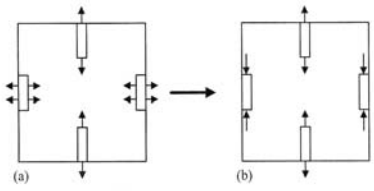

Figure 2 – Directions of tensile forces on the resistors for the applied pressure.

If there is pressure on the membrane, then both the length of *R1* and *R3* become larger, and so do the resistances of which. One the contrary, the width of *R2* and *R4* are increased, so that the resistances of which become smaller. By this way the output voltage of the bridged-circuit is as follows:

$$V_{out} = (\frac{R_3}{R_3 + R_4} - \frac{R_2}{R_1 + R_2})V_o \quad (1)$$

where

$$R_1 = R_3 = R_0 + \Delta R_1$$
$$R_2 = R_4 = R_0 + \Delta R_2 \quad (2)$$

By equations (1) and (2), one has:

$$\frac{V_{out}}{V} = \frac{R_0+\Delta R_1}{R_0+\Delta R_1+R_0+\Delta R_2} - \frac{R_0+\Delta R_2}{R_0+\Delta R_1+R_0+\Delta R_2} = \frac{\Delta R_1-\Delta R_2}{2R_0+\Delta R_1+\Delta R_2} \quad (3)$$

In general, $R_0 >> \Delta R_1 (=R= -\Delta R_2)$, then $\frac{V_{out}}{V_0} = \frac{\Delta R}{R} = k\varepsilon P$, (4)

where P –means the pressure,
K –means the Gauge Factor,
ε –means the strain.

Thus one can obtain the pressure by detecting the voltage output.

3 PRESSURE SENSOR TESTER DESIGN

3.1 Driver circuit design

If one use a constant voltage source driver as shown in Fig. 3, and only *R3* becomes larger, i.e., $R_3 = R + \Delta R$, then, the output voltage is

$$V_o = \frac{R_3}{R_3 + R_4} \times V_{ref} - \frac{R_2}{R_1 + R_2} \times V_{ref}$$
$$= \frac{R + \Delta R}{(R + \Delta R) + R} V_{ref} - \frac{R}{R + R} V_{ref} \quad (5)$$
$$V_o = \frac{R + \Delta R}{2R + \Delta R} V_{ref} - \frac{1}{2} V_{ref} = \frac{\Delta R}{4R + 2\Delta R} V_{ref}$$

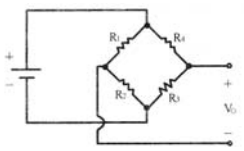

Figure 3 – Constant voltage source driver.

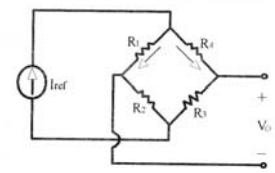

Figure 4 – Constant current source driver.

On the contrary if one use a constant current source driver as shown in Fig. 4, then similar to the above derivation, one has:

$V_o = I_2 R_3 - I_1 R_2 = (I_2 - I_1) \times R$, where

$$I_2 = \frac{(R_1+R_2)}{(R_1+R_2)+(R_3+R_4)} \times I_{ref} = \frac{2R}{4R+\Delta R} \times I_{ref} \quad (7)$$

$$I_1 = \frac{(R_3 + R_4)}{(R_1 + R_2) + (R_3 + R_4)} \times I_{ref} = \frac{2R + \Delta R}{4R + \Delta R} \times I_{ref} \quad (8)$$

then $V_o = (I_2 - I_1) \times R = \frac{\Delta R}{4R + \Delta R} \times R \times I_{ref}$, (9)

From the above derivation, one can see that the condition defined by the inequality equation ($4R >> \Delta R$) is stronger than that defined by $2R >> \Delta R$, so that not only the accuracy, but also the linearity of the tester are better by using the current source as the driver.

In general, the output voltage of the pressure sensor can be expressed as:

$$V_o = S \times P \times V_B \pm V_{OS} \quad (10)$$

where V_o –means the output voltage (mV),
S –means the sensitivity (mV/V/psi),
P –means the applied pressure (psi),
V_B –means the voltage across the bridge circuit,
V_{OS} –means the offset voltage with P=0.

3.2 Temperature error effects

In general, there are three types of temperature errors:
(1) *TCS* (Temperature Coefficient of Span): typical values -2000~-3000 PPM/°C
(2) *TCO* (Temperature Coefficient of Offset): typical values 0~10 μV/V/°C
(3) *TCR* (Temperature Coefficient of Resistor): typical values +500 ~ +1000 PPM/°C,
These variables are defined as:

$$TCS = \frac{\dot{S}}{S} \qquad \dot{S} = \frac{Change\ in\ Span}{Change\ in\ Temperature}$$

$$TCR = \frac{\dot{R}}{R} \qquad \dot{R} = \frac{Change\ in\ \mathrm{Re}sistor}{Change\ in\ Temperature}$$

where S –means the pressure span,
R –means the bridge resistor (R_B).

3.3 Temperature compensation method

According to the presence of the applied pressure, there are two types of error sources:
(1) Temperature Errors of Span (with pressure applied)
(2) Temperature Errors of Bias V_{OS} (without pressure applied)

In order to eliminate these errors, it's necessary to compensate the errors one by one, firstly for the span temperature compensation as follows:

By equation (10) one has $V_o = S \times P \times V_B \pm V_{OS}$ if V_{OS}=0, then $V_o = S \times P \times V_B$

Followings are the trade-offs of voltage or current source driver:

(1) Voltage Source Driver

In this case the bridge drive-voltage *VB* is *Vs.* Since Vs is a constant voltage source, i. e.,

$$V_o = S \times P \times V_S \qquad (V_S = Const)$$

then $\dot{V}_o = P \times V_S \times \dot{S}$, and $\frac{\dot{V}_o}{V_o} = \frac{P \times V_S \times \dot{S}}{P \times S \times V_S} = \frac{\dot{S}}{S}$ $(\frac{\dot{S}}{S} = TCS)$ (11)

Thus in this case the temperature coefficient of output voltage is *TCS*.

(2) Current Source Driver

In this case the current source *I* is a constant, then the bridge drive voltage *VB* is

$$V_B = I \times R_B$$

$$V_o = P \times S \times I \times R_B \qquad (12)$$

Since I is a constant, only R_B and *S* are functions of temperature, by equation (12) one has

$$V_o = P \times I \times S \times R_B$$

$$\dot{V}_o = P \times I(R_B \dot{S} + S \dot{R}_B)$$

$$\frac{\dot{V}_o}{V_o} = \frac{P \times I(R_B \dot{S} + S \dot{R}_B)}{P \times I \times S \times R_B}$$

or $\frac{\dot{V}_o}{V_o} = \frac{\dot{S}}{S} + \frac{\dot{R}_B}{R_B}$ (13)

Thus in this case the temperature coefficient of output voltage is the sum of *TCS* and *TCR*. For ideal case of compensation one has:

$\frac{\dot{V}_o}{V_o} = 0$

i. e., $\frac{\dot{S}}{S} = -\frac{\dot{R}_B}{R_B}$ (14)

or $TCS = -TCR$ (15)

Thus this is the guide of our choice, *e. g.,* if TCS = -2000 PPM/°C, then one should use TCR = +2000 PPM/°C, and $\frac{\dot{V}_o}{V_o} = \frac{\dot{S}}{S} + \frac{\dot{R}_B}{R_B} = -2000 + 2000 = 0$

Should one use voltage source as the driver, then a thermistor is needed as shown in Fig. 5. By equation (10) if one let V_{OS}=0, then $V_o = S \times P \times V_B$ and $\dot{V}_o = P \times (V_B \dot{S} + S \dot{V}_B)$

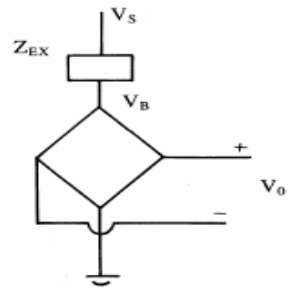

Figure 5 – A thermistor is needed by using voltage source driver.

Thus one has $\frac{\dot{V}_o}{V_o} = \frac{P \times (V_B \dot{S} + S \dot{V}_B)}{P \times S \times V_B} = \frac{\dot{V}_B}{V_B} + \frac{\dot{S}}{S}$ (16)

Since $V_B = \frac{V_S}{R_B + Z_{EX}} \times R_B$ (17)

then one has $\frac{\dot{V}_B}{V_B} = \frac{Z_{EX}}{R_B + Z_{EX}} (\frac{\dot{R}_B}{R_B} - \frac{\dot{Z}_{EX}}{Z_{EX}})$ (18)

By equations (16) and (18) one has

$$\frac{\dot{V}_o}{V_o} = \frac{\dot{S}}{S} + \frac{Z_{EX}}{R_B + Z_{EX}} (\frac{\dot{R}_B}{R_B} - \frac{\dot{Z}_{EX}}{Z_{EX}}) \quad (19)$$

For ideal case of compensation one has: $\frac{\dot{V}_o}{V_o} = 0$

which yield $\frac{\dot{S}}{S} = -\frac{Z_{EX}}{R_B + Z_{EX}} (\frac{\dot{R}_B}{R_B} - \frac{\dot{Z}_{EX}}{Z_{EX}})$ (20)

If $Z_{EX} = R$, then equation (20) can be re-written as:

$\frac{\dot{S}}{S} = -\frac{R}{R_B + R} (\frac{\dot{R}_B}{R_B} - \frac{\dot{R}}{R})$ (21)

and if R is with positive coefficient, and in general case, TCS is a negative value, thus one has the following condition for ideal compensation: $|TCR_B| > |TCS|$

But in general case, TCR_B is less than TCS, thus it's not practical to use a positive coefficient resister for temperature compensation. Thus one should use a negative coefficient one,

i. e., a thermistor, with $Z_{EX} = R$, then one yield $\frac{\dot{S}}{S} = -\frac{R_T}{R_B + R_T} (\frac{\dot{R}_B}{R_B} - \frac{\dot{R}_T}{R_T})$ (22)

If TCS = -2800 PPM/°C, and $TCR_B = 800$ PPM/°C, by equation (22) one has

$-2800 = -(0.5)(800 - \frac{\dot{R}_T}{R_T})$

thus in order for ideal compensation $\frac{\dot{V}_o}{V_o} = 0$, one has TCR_T = -4800PPM/°C

4 SMART PRESSURE SENSOR MODULE REALIZATION

According to the smart sensor module architecture defined by IEEE 1451 Standard as shown in Fig. 6, in which there are two parts as follows:

(1) Smart Transducer Interface Module, STIM (IEEE 1451.1)

(2) Network Capable Application Processor, NCAP (IEEE 1451.2)

In the first part, there are A/D, D/A, digital I/O as well as addressing circuits, but in this special experiment topic, one need A/D and addressing circuits. While in the second part, there are micro-processor as well as transceiver for network interconnection, which can be accomplished by using a 8051 micro-computer. Thus the resulting smart pressure sensor module is shown in Fig. 7, in which the differential inputs of the low drift instrumentation amplifier (IA, TL074) as shown in Fig. 7, is used to match up with the bridge differential outputs. The other benefits are the impedance match, offset compensation as well as gain control. The output voltage of IA is derived as follows

$$V_{O3} = (V_2 - V_1)(1 + \frac{2R_2}{R_1})(\frac{R_4}{R_3})$$

$$= V_S(1 + \frac{2R_2}{R_1})(\frac{R_4}{R_3})$$

Following IA, a twelve bits A/D (AD574A) is used to convert the analog signal into a digital one. Finally, the block diagram as well as circuit layout of the pressure sensor module are shown in Figures 8 and 9.

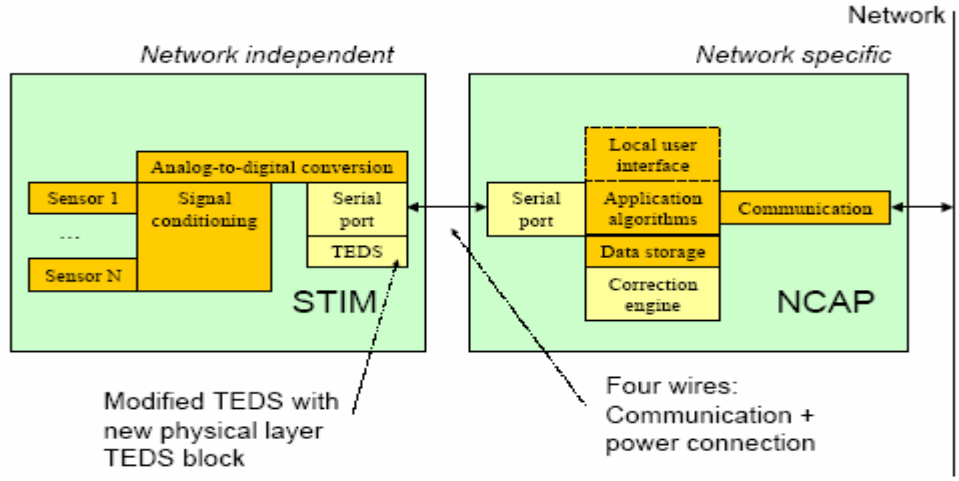

Figure 6 – Architecture of IEEE 1451 standard for smart sensor module.

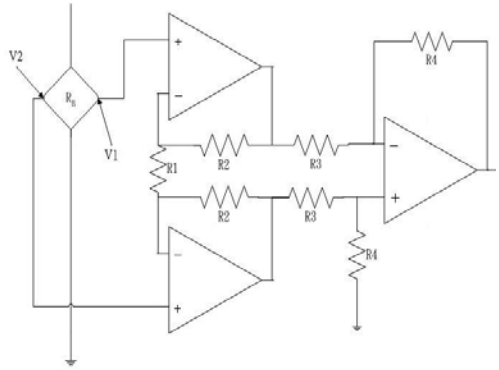

Figure 7 – The block diagram of instrumentation amplifier.

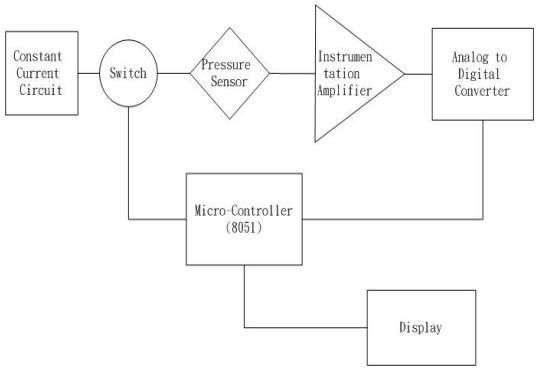

Figure. 8 – The block diagram of the pressure sensor module.

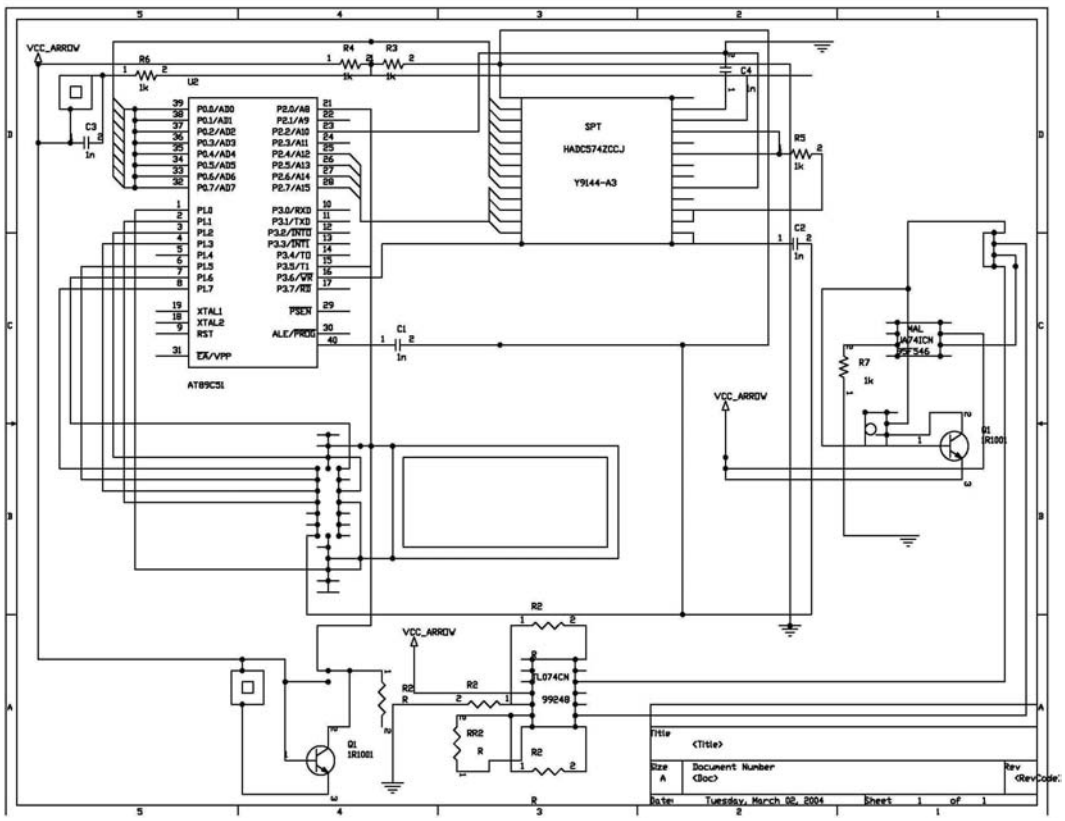

Figure 9 – Circuit layout diagram of the whole module

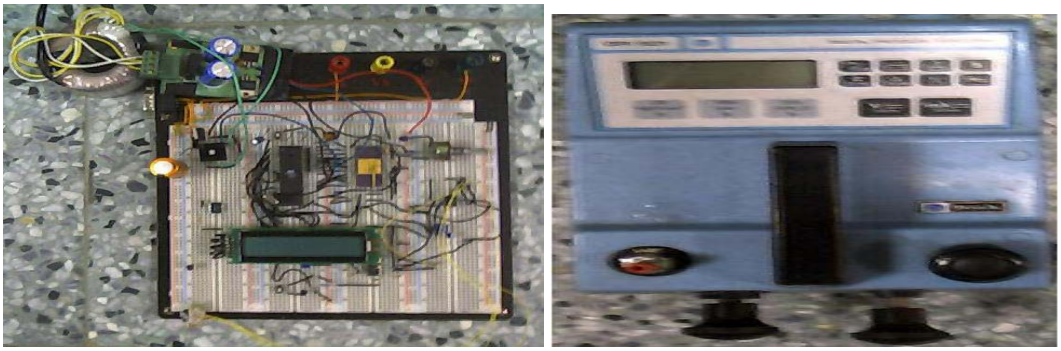

Figure 10 – (a) Practice- board of the experiment and, (b) Digital pressure readings on a LCD display.

It should be noted that in order to avoid the sensor heating effect, the current source (1.5 mA) in Fig. 9 is a pulsed-type with the duration of stabilization time as 1ms. The practice-board of the experiment as well as the final readings on a LCD display are shown in Fig. 10 (a) and (b).

5 EXPERIMENT RESULTS AND DISCUSSIONS

The pressure is supplied by a source named Digital Pressure Indicator (Druck DPI601). The temperature of the oven is from –20 °C to 100 °C. The output voltage in mV for various temperatures and pressures are shown in Table 1 and Figs.11 and 12. The scale factors for various temperatures are also shown in Table 2 and Figure 13.

Table 1. Output-voltage in mV for various temperatures and pressures.

	0psi	5psi	10psi	15psi	20psi	25psi	30psi	35psi	40psi	45psi	50psi
-20℃	13.5	27.2	41.1	54.7	68.6	82.4	96.1	110.1	124	137.7	151.8
-10℃	12.8	26.7	40.8	54	67.1	81.5	94.7	108.6	122.7	136.4	150.1
0℃	12.5	25.7	39.3	52.7	66.2	79.9	93.5	107.1	120.7	134.3	147.9
10℃	11.6	25.1	38.5	51.9	65.5	78.8	92.3	105.8	119.2	132.8	146.6
20℃	11.1	24.5	37.9	51.3	64.8	78.3	91.9	105.6	119	132.7	146.4
30℃	10.3	23.8	37.2	50.7	64	77.3	91	104.4	118	131.3	145
40℃	10.3	23.8	37	50.4	63.7	76.9	90.4	103.8	117.2	130.6	144.3
50℃	10.3	23.7	36.9	50.3	63.6	76.7	89.9	103.3	116.7	130	143.5
60℃	10.1	23.5	36.7	49.9	63.2	76.6	89.6	102.7	116	129.3	142.7
70℃	9.9	23.3	36.4	49.5	62.8	76	89.2	102.5	115.6	128.8	142.2
80℃	9.7	23.1	36.2	49.4	62.4	75.6	88.8	102.2	115.2	128.3	141.6
90℃	9.6	22.8	35.9	49.1	62.3	75.4	88.5	101.7	114.9	127.8	141.3
100℃	9.6	22.5	35.6	48.8	61.9	75.2	88.2	101.5	114.6	127.6	140.9

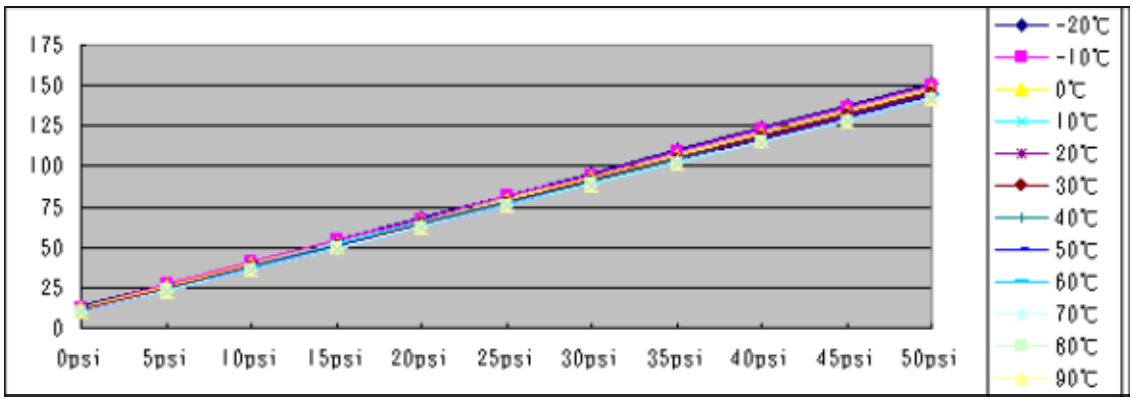

Figure 11 – Output-voltage in mV vs. pressure for various temperatures.

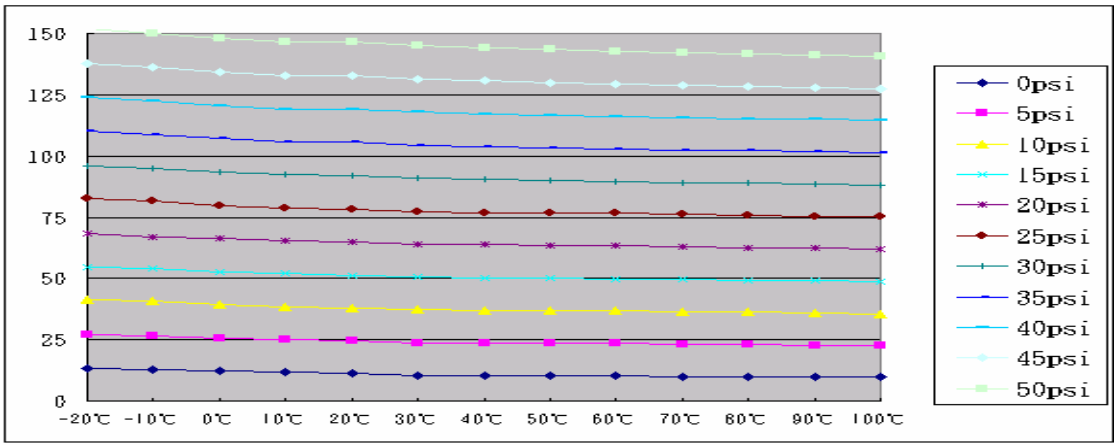

Figure 12 – Output-voltage in mV vs. temperature for various pressures.

By using the values such as biases and scale factors, one has the compensated results as well as the percentage errors are also shown in Tables 3 and 4. It can be seen that the maximal error is 1,64 %, which is less than 2 %, that is the acceptable tolerance of the commercial specification.

Table 2. Scale factors for various temperatures.

Temperatures	-20℃	-10℃	0℃	10℃	20℃	30℃	40℃	50℃	60℃	70℃	80℃	90℃	100℃
Scale factors	0.363	0.366	0.370	0.372	0.373	0.374	0.375	0.376	0.377	0.378	0.379	0.380	0.382

Scale Factors

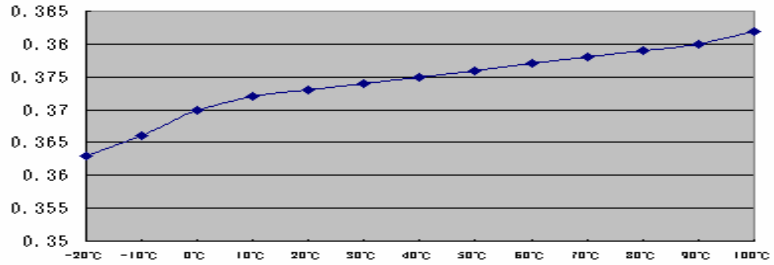

Figure 13 – Scale factors for various temperatures.

Table 3. Compensated results for various pressures and temperatures.

	0psi	5psi	10 psi	15 psi	20 psi	25 psi	30 psi	35 psi	40 psi	45 psi	50 psi
-20℃	0	4.994	10.060	15.0174	20.084	25.114	30.1077	35.2107	40.277	45.2709	50.414
-10℃	0	5.1013	10.276	15.1204	19.9281	25.2129	30.0573	35.1586	40.3333	45.3612	50.3891
0℃	0	4.9513	9.94	14.891	19.879	24.941	29.966	34.992	40.0169	45.042	50.0673
10℃	0	5.022	10.007	14.9916	20.0508	24.9984	30.0204	35.0424	40.0272	45.0864	50.22
20℃	0	4.9982	9.996	14.9946	20.0301	25.0656	30.1384	35.2485	40.2467	45.3568	50.4669
30℃	0	5.049	10.061	15.1096	20.0838	25.058	30.1818	35.1934	40.2798	45.254	50.3778
40℃	0	5.0625	10.013	15.0375	20.025	24.975	30.0375	35.0625	40.0875	45.1125	50.25
50℃	0	5.0384	10.002	15.04	20.0408	24.9664	29.9296	34.968	40.0064	45.0072	50.0832
60℃	0	5.0518	10.03	15.0046	20.0187	25.0705	29.9715	34.9102	39.9243	44.9384	49.9902
70℃	0	5.0652	10.017	14.9688	19.9962	24.9858	29.9754	35.0028	39.9546	44.9442	50.0094
80℃	0	5.0786	10.044	15.0463	19.9733	24.9761	29.9789	35.0575	39.9845	44.9494	49.9901
90℃	0	5.016	9.994	15.01	20.026	25.004	29.982	34.998	40.014	44.916	50.046
100℃	0	4.9149	9.906	14.9352	19.9263	24.9936	29.9466	35.0139	40.005	44.958	50.0253

Table 4. The %error of the compensated results for various pressure and temperature.

	0psi	5psi	10 psi	15 psi	20 psi	25 psi	30 psi	35 psi	40 psi	45 psi	50 psi
-20℃	0	1.64%	0.188%	0.296%	0.007%	0.043%	0.054%	0.188%	0.279%	0.188%	1.64%
-10℃	0	1.016%	0.65%	0.528%	0.631%	0.577%	0.082%	0.179%	0.559%	0.528%	1.016%
0℃	0	0.84%	0.47%	0.59%	0.47%	0.1%	0.023%	0.111%	0.178%	0.229%	0.84%
10℃	0	0.44%	0.068%	0.056%	0.254%	0.006%	0.068%	0.121%	0.068%	0.192%	0.44%
20℃	0	0.036%	0.036%	0.036%	0.151%	0.262%	0.461%	0.71%	0.617%	0.793%	0.036%
30℃	0	0.232%	0.606%	0.731%	0.419%	0.232%	0.606%	0.553%	0.7%	0.564%	0.232%
40℃	0	0.5%	0.125%	0.25%	0.125%	0.1%	0.125%	0.179%	0.219%	0.25%	0.5%
50℃	0	0.768%	0.016%	0.267%	0.204%	0.134%	0.235%	0.091%	0.016%	0.016%	0.768%
60℃	0	0.282%	0.282%	0.031%	0.094%	0.282%	0.095%	0.257%	0.189%	0.137%	0.282%
70℃	0	0.548%	0.17%	0.208%	0.019%	0.057%	0.082%	0.008%	0.114%	0.124%	0.548%
80℃	0	0.814%	0.435%	0.309%	0.134%	0.096%	0.070%	0.164%	0.039%	0.112%	0.814%
90℃	0	0.32%	0.06%	0.067%	0.13%	0.016%	0.06%	0.006%	0.035%	0.187%	0.32%
100℃	0	0.784%	0.784%	0.275%	0.212%	0.132%	0.021%	0.197%	0.17%	0.064%	0.784%

ACKNOWLEDGEMENTS

This work was supported by Ministry of Education of the Republic of China under the grant of 2003 teaching performance improvement programs in the fields of Precision Machinery Measurement and Micro Avionics.

REFERENCES

BURGER, G. J., LAMMERINK, T. S. J. J., FLUINTMAN H. J., IMAI, S., TOKUYAMA, M., & HIROSE, S., 1995. *Piezoelectric impact force sensor array for tribology research on rigid disk storage media*, Micro Electro Mechanical Systems, MEMS '95, Proc. IEEE, 6 s.

CHUNG, G., KAWAHITO, S., ISHIDA, M., & NAKAMURA, T., 1990. *Novel pressure sensors with multilayer SOI Structure*, Electronics Letters, 26,3 s.

COZMA, A., PUERS, R. 1997. *Electrostatic actuation as a self-testing method for silicon pressure sensor*, Sensors and Actuators, A 60, 4 s.

DELIC, N., VUJANIC, A. DETTER, H., DJURIC, Z., SIMICICI, N., and PETROVIC, R., 1997. *Piezo-resistive force sensor developed for use in handling of micro-parts*, IEEE Microelectronics, 1997 Proceedings, 1997 21st International, 4 s.

FUKANG, J., TAI, C., WALSH, W., TOM, T., LEE, G., & HO, C., 1997. *A flexible MEMS technology and its first application to shear stress sensor skin*, IEEE, MEMS-97, 6 s.

GUCKEL, H., and BURNS, D., 1984. *Planar Processed Poly-silicon Sealed Cavities for Pressure Transducers Array*, IEDM, 3 s.

KALVESTEN, E., 1998. *The first surface micro-machined pressure sensor for cardiovascular pressure measurements*, IEEE MEMS-98, 5 s.

KIM, H., JEONG, Y., and CHUN, K., 1997. I*mprovement of the linearity of a capacitive pressure sensor using an interdigited electrode structure*, Sensors and Actuators A 62, 5 s.

LEE, C., and SUGA, I., 1996. *Micro-machined piezoelectric force sensors based on PZT thin films*, Ultrasonics, Ferroelectrics and Frequency Control, IEEE , T. Res. Center for Adv. Sci. & Technol., Tokyo Univ., 7 s.

LEE, C., TOH, T., MAEDA, I., & SUGA, T., 1996. *Smart force sensors for scanning force microscope using the micro-machined piezoelectric PZT cantilevers,* IEEE Electron Devices Meeting, International, 5 s.

PANDIAN, T., KUDA, O. MITANI, Y., KURASHI, K., and KAWAMURA, S., 1995. *A piezoelectric force / force- derivative sensor for robotic applications*, SICE ' 95, Proceedings of the 34th SICE Annual Conference, International Session Papers, 3 s.

PETERSON, K., 1982. *Silicon as a mechanical material,* Proceedings of IEEE, 70.5,. 4 s.

PUERS, R., DE BRUYKER, D., and COZMZ, A., 1997. *A novel combined redundant pressure sensor with self-test function,* Sensors and Actuators, A 60, 4 s.

Reinhart, R., *Calibration Visualization and Automation Software for IEEE 1451.2 Compliant Smart Sensors.*

SUSUMU, S., & SHIMAKODA, K., 1991. *Surface micro-machined micro-diaphragm pressure sensors*, Solid-State Sensors and Actuators, 4 s.

YOSHIDA, K., TANIGAWA, H., *1989.Development of a force sensor for minute load measurement,* Electronic Manufacturing Technology Symposium, 1989, Proc. Japan IEMT Symposium, Sixth IEEE/CHMT International, 1989, 4s.